Numerical assessment for robustness of push-pull fume cupboard

Ming-Jyh Chern and Chi-Yeh Lee

Department of Mechanical Engineering
National Taiwan University of Science and Technology
Taipei 10607, Taiwan. E-mail: mjchern@mail.ntust.edu.tw

ABSTRACT

A push-pull fume cupboard is a device to capture chemical vapors in a laboratory or a factory. It utilizes a push flow from the bottom of the sash and a pull flow behind the doorsill to form an air curtain and capture pollutants inside the cupboard. The effects of arms and walk-by on the capture flow in the push-pull fume cupboard are not clear. Hence, this study is aimed on evaluation of the influences of arms and walk-by on the fume cupboard using a numerical model for turbulent flow. In terms of predicted results, the push-pull fume cupboard is not affected by arms. To avoid the walk-by effect, the ratio of push and pull flow speeds has to be adjusted to a specified region.

1. INTRODUCTION

A fume cupboard is a common local ventilation device to isolate and remove toxic vapors from an indoor laboratory. The push-pull air curtain technique has been adopted in capture of pollutants coming from an open surface tank with a large area. Its relevant studies can be found in several references such as Malin (1945), Battista (1947), Hama (1957), Robinson & Ingham (1995a, b), Rota *et al.* (2001), Huang *et al.* (2005), and Chern & Ma (2006). A push-pull fume cupboard utilizing an air curtain as the capture flow between the sash and doorsill has been proposed by Huang *et al*. (2005) and Chern & Cheng (2007) as shown in Fig. 1 and compared with an exhaust fume cupboard which uses a fan at the roof to generate a capture flow. According to their results, a push-pull fume cupboard effectively reaches the purpose with or without an operator in front of a fume cupboard. The concave curtain mode which utilizes a weak push flow from the bottom of the sash and a strong pull flow behind the doorsill is recommended in the operation of the push-pull fume cupboard.

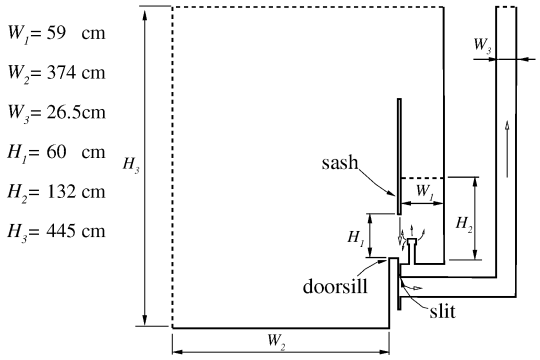

Fig. 1 Schematic of a push-pull fume cupboard.

The aim of this study is to further investigate the robustness of the push-pull fume cupboard under two various situations. First, an operator's arms intruding the air curtain are employed. The operator's walk by the fume cupboard is then examined. An operator is located at the right hand side of the opening in the beginning of the simulation. It moves suddenly at the speed 1 m/s toward the left hand side. It takes two seconds to pass the cupboard and then stops in the left hand side of the opening. In order to observe the robustness, a variety of push and pull speeds are considered. To predict the distribution of toxic vapor, SF_6 is considered as a tracer gas in the model

according to the standard of ASHRAE (1995). 3-D streamlines and distributions of SF_6 are presented to observe the influences of those situations.

2. MATHEMATICAL FORMULAE AND NUMERICAL MODEL

A fluid shall conserve mass and momentum in a flow. As a result, the continuity equation and Navier-Stokes equations are mathematic forms of those conservation laws. Moreover, the air flow caused by a fume cupboard is turbulent. In order to simulate the turbulent air flow, Reynolds's decomposition is applied to the continuity and Navier-Stokes equations denoted as

$$\frac{\partial U_j}{\partial x_j} = 0, \qquad j = 1, 2, 3 \tag{1}$$

and

$$\rho\left[\frac{\partial U_i}{\partial t} + \frac{\partial (U_i U_j)}{\partial x_j}\right] = -\frac{\partial P}{\partial x_i} + \frac{\partial}{\partial x_j}\left(\mu \frac{\partial U_i}{\partial x_j} - \rho\overline{u_i' u_j'}\right), \quad i, j = 1, 2, 3 \tag{2}$$

where U_j is a mean velocity component, P is the mean pressure, ρ is the density of the fluid, and μ is the dynamic viscosity of the fluid. It is found that new variables, $-\rho\overline{u_i' u_j'}$, called the Reynolds stresses appear in Eq. (2). It requires more equations to solve components of Reynolds stress, so we employ the standard k-ε turbulence model to determine Reynolds stress. More details regarding this part can be found in Chern and Cheng (2007).

The turbulent mass transfer equation based on Reynolds' decomposition approach is used to explore concentration variations and is denoted as

$$\frac{\partial C}{\partial t} + \frac{\partial U_j C}{\partial x_j} = \frac{\partial}{\partial x_j}\left(D_m \frac{\partial C}{\partial x_j} - \overline{u_j' c'}\right), \quad j = 1 \sim 3 \tag{3}$$

where C and c' are the temporal mean and fluctuating value of concentration, respectively. The concentration fluctuation term $-\overline{u_j' c'}$ is proportional to the concentration gradient, i.e.,

$$-\overline{u_j' c'} = D_t \frac{\partial C}{\partial x_j}, \tag{4}$$

where D_t is the turbulent diffusion coefficient. Since turbulent flows are complex and highly changeable, regarding D_t as a constant is usually unreliable for most applications. Therefore, we adopt the turbulent Schmidt number (Sct) defined as the ratio of the turbulent momentum diffusion rate to the turbulent mass diffusion rate, i.e. μ_t/D_t. The turbulent Schmidt number relates to the ratio of the viscous diffusion to mass diffusion, and can be assumed as a constant. Depending on the situation under consideration, this value will vary from 0.8 to 1.2 (see Durst and Pereira, 1991). We use Sct = 1 for the following studies. SF_6 is used as a tracer gas in the numerical model. Its density and molecular diffusivity in air are 6.04 kgm^{-3} and $3x10^{-5}$ m^2s^{-1}.

Cartesian grids are used to discretize the whole 3-D flow field. Fig. 2 reveals the vertical central plane of the mesh. Grids are refined in the vicinity of the fume cupboard. 545,727 grids are employed in the model. The grid independence test is performed. Due to page limit, the result of grid independence test is not shown in this manuscript.

A quiescent flow field is used as the initial condition in the model. Simulations do not terminate until steady state solutions are reached. For each steady solution, the ratio of the maximum temporal variation of velocity to its magnitude is less than 10^{-4}. The software STAR-CD™ based on the finite volume method is employed to solve Eqs. (1)-(3). The 2nd order Crank-Nicolson scheme and the QUICK scheme are used for the temporal and advective terms, respectively. The PISO scheme is utilized for the pressure-velocity iteration. The maximum mass residual from all computational cells must be less than 10^{-5}.

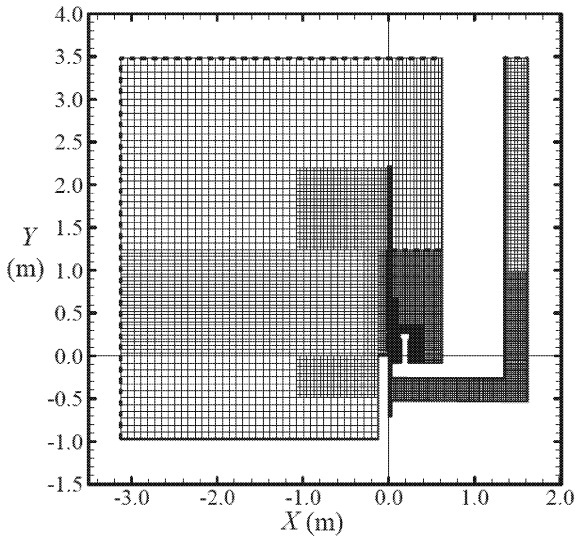

Fig. 2 The central vertical plane of the utilized mesh for the push-pull fume cupboard.

3. RESULTS AND DISCUSSION

Effect of Arms

The effect of arms is evaluated first in the study. Two arms of the operator intrude the air curtain horizontally. Figs. 3 (a)-(d) show the streamline patterns of vertical planes above the doorsill inside the fume cupboard under the effect of arms, but Figs. 3 (e)-(h) present the results without arms. It is found that the air curtain generated by the push and pull flows is not affected by the intruding arms. Moreover, concentration contours of SF_6 are shown in Fig. 4 in which (a)-(c) and (d)-(f) are results with and without arms, respectively. It is revealed that pollutants are confined between two arms as shown in Figs. 4 (a)-(c). That means the effect of intruding arms is not negative, but positive in the capturing capability of the fume cupboard.

The effect of arms is further examined using 3-D isosurfaces of SF6 in an exhaust and the push-pull fume cupboards. Fig. 5 shows 3-D isosurfaces of SF6. Sub-figures (a) and (b) show results for the exhaust fume cupboard. It is found that all pollutants are accumulated inside the cupboard. The maximum concentration higher than 10 ppm in Figs. 5 (a) and (b) is located in front of the operator. As a result, the cupboard does not protect the operator. The details can be found in Chern and Cheng (2007). On the other hand, pollutants are effectively removed by the pull flow inside the push-pull fume cupboard as shown in Figs. 5 (c) and (d). There is not accumulation of pollutant in front of the operator. Also, the effect of arms dose not make the capturing capability of the air curtain worse in the push-pull fume cupboard.

Effect of Walk-by

The other important effect for the performance of a fume cupboard is the effect of walk-by. If one walks in front of the cupboard, then it may influence the air flow inside the cupboard. Fig. 6 presents the schematic of the problem. An operator walks at 1 m/s from the right hand side to the left hand side. The motion takes 2 seconds. In the simulations, it takes 20 seconds for the air flow to reach a steady state inside the push-pull fume cupboard. The operator starts to walk at t = 20 seconds. The example using the push flow at 3 m/s and the pull flow at 14 m/s is demonstrated. Fig. 7 reveals flow variations of the horizontal planes 15 and 40 cm above the doorsill. It can be found that a vortex is formed between the operator and the fume cupboard during the first second of the walk. However, the vortex does not influence the air curtain for a long time. The air curtain recovers after the operator walk by the cupboard. Fig. 8 shows the 3-D streamline plots. The vortex can be seen at t = 21.2 and 21.9 seconds, but it disappears gradually after the operator walks by the cupboard. Subsequently, the air curtain retrieves the concave mode.

Furthermore, we examine distributions of SF_6 concentration inside the fume cupboard. Fig. 9 shows the transient variation of the concentration isosurface at 0.1 ppm when an operator walks by. Due to the vortex as the operator approaches the opening, a small amount of pollutants leak (see subfigures for t = 21.6 to 23 seconds). Nevertheless, the leak of

pollutants does not disperse after the operator stops. Since the air curtain goes back to the concave mode again after the operator stops, the leak of pollutants is sucked by the recovered air curtain as shown in the subfigure at t = 26 seconds. In additions, we investigate time histories of concentration at 12 various points on the opening as shown in Fig. 11. If the value of concentration is higher than 0.1 ppm, then it exceeds the required criterion. In Fig. 10, only the concentration at Point 11 is instantaneously higher than 0.1 ppm at t = 21 seconds, but it is decreased quickly after t = 21 seconds. Apparently, it is due to the vortex shown in Fig. 8, because Point 11 is the place of the vortex inception. In terms of those predicted results, it turns out that the push-pull fume cupboard is robust under the effect of walk-by. A variety of push and pull flow speed combinations are examined using the time histories of concentration at 12 points.

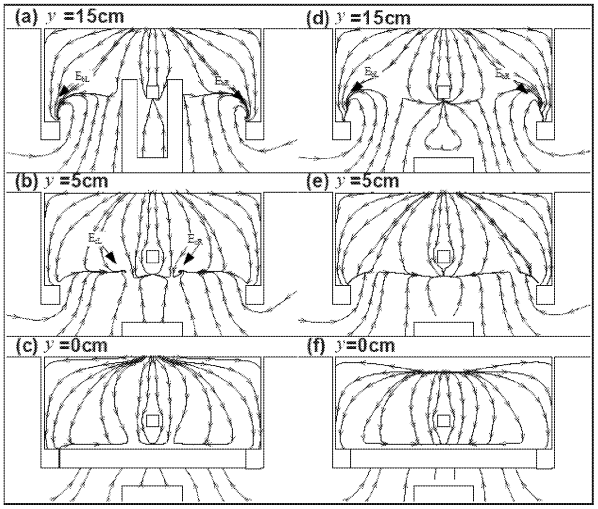

Fig. 3 Streamline patterns of horizontal planes side the fume cupboard. (a)-(c) with arms. (d)-(f) without arms. The push and pull speed are 0.5 and 9 m/s, respectively.

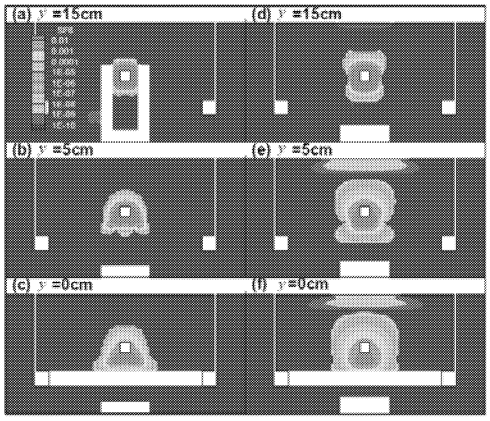

Fig. 4 Concentration contours of SF6 of horizontal planes side the fume cupboard. (a)-(c) with arms. (d)-(f) without arms. The push and pull speed are 0.5 and 9 m/s, respectively.

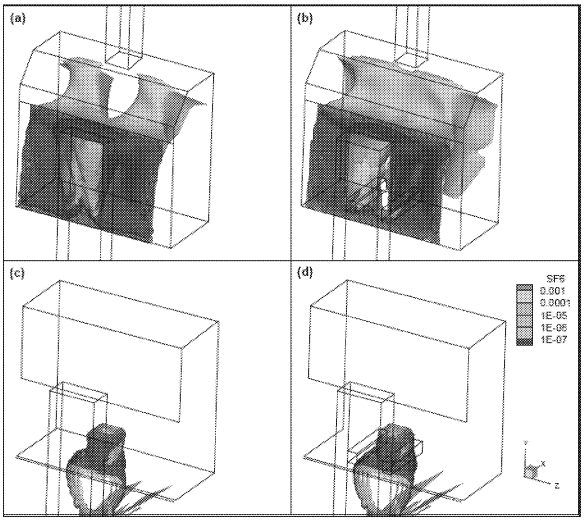

Fig. 5 Isosurfaces of SF_6. (a) and (b) are results for an exhaust fume cupboard with and without arms. (c) and (d) are results for the push-pull fume cupboard with and without arms.

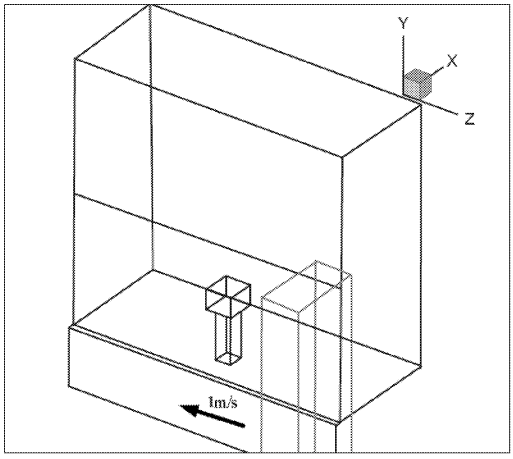

Fig. 6 Schematic of assessment of walk-by effect.

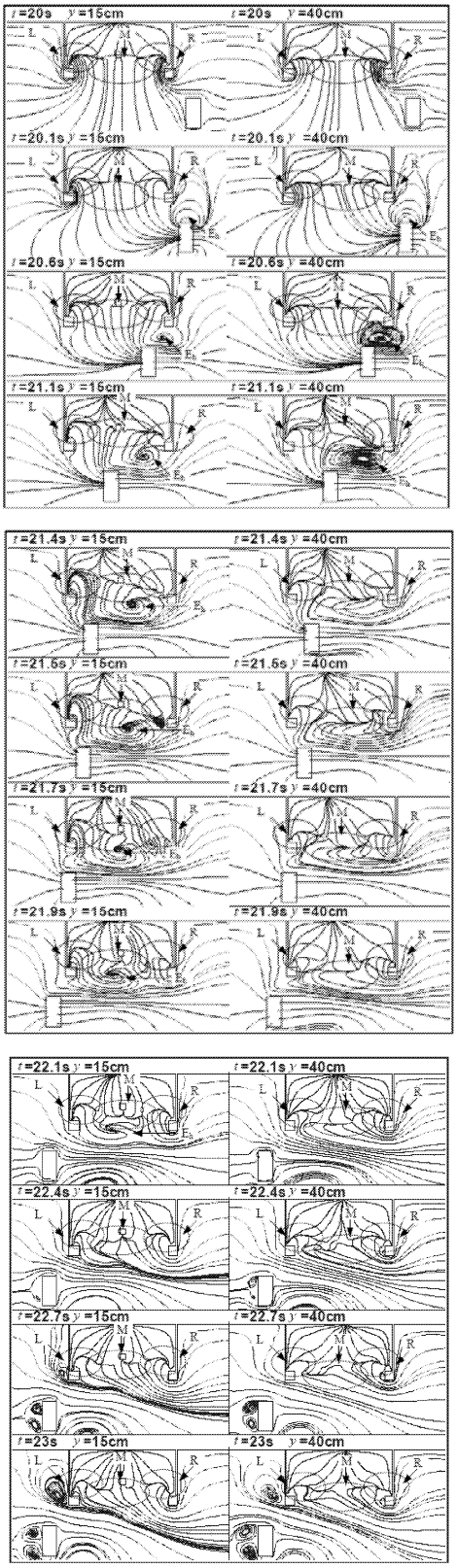

Fig. 7 Flow variations of two horizontal planes 15 and 40 cm above the doorsill. Speeds of push and pull flows are 3 and 14 m/s, respectively.

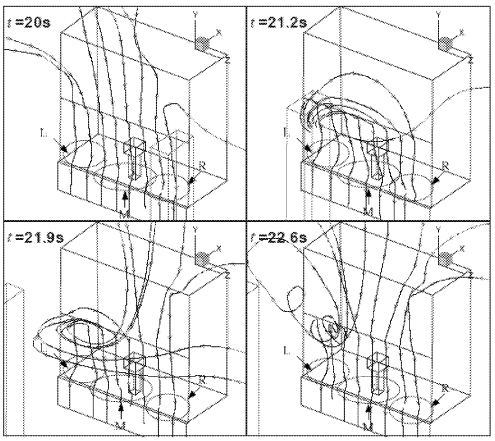

Fig. 8 3-D streamline plots of walk-by effect. Speeds of push and pull flows are 3 and 14 m/s, respectively.

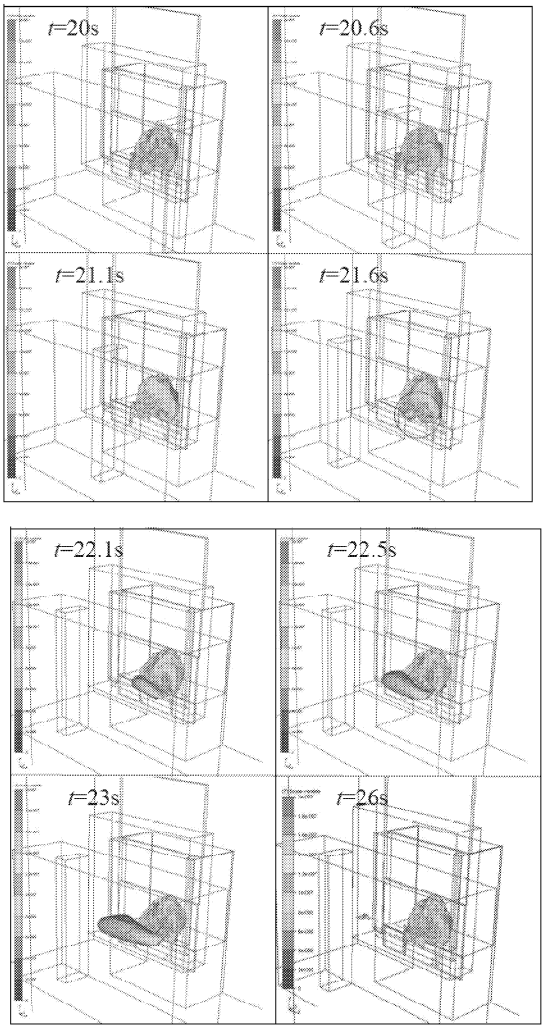

Fig. 9 The temporal variation of iossurface at 0.1 ppm under the effect of walk-by. Speeds of push and pull flows are 3 and 14 m/s, respectively.

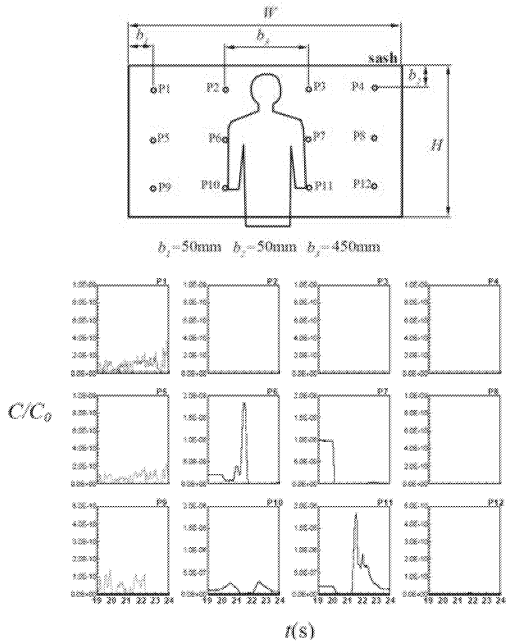

Fig. 10 Time histories of concentration at 12 points of the opening.

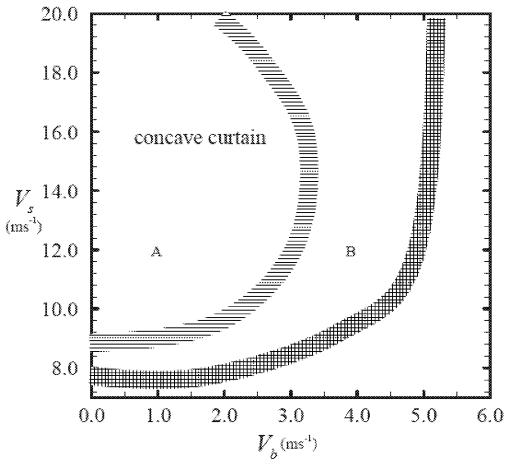

Fig. 11 Recommended combinations of push and pull flow speeds. Part A is robust, but Part B may have a small amount of leakage.

Fig. 11 presents the recommended operation region. Part A in Fig. 11 refers to the very robust concave mode, no leak of pollutants disperses. In Part B, there is a very small amount of leak which between 0.1 ppm and 1 ppm may occur under the effect of walk-by. Hence, it is suggested to use the Part A as the operation for the push-pull fume cupboard.

4. CONCLUSIONS

The push-pull fume cupboard is examined by the effects of arms and walk by. In the investigation of intruding arms, the capability of capturing pollutants for a push-pull fume cupboard is enhanced when arms intrude the air curtain formed by the push and pull flows. Furthermore, when an operator walks by the fume cupboard, a vortex is formed between the operator and the opening of the cupboard. When the operator walk by the fume cupboard and stops, the vortex disappears and does not destroys the air curtain. Although the air curtain is disturbed by the vortex, the air curtain recovered very soon when the operator stops. According to the predicted results of concentration, the air curtain is very robust under the walk-by effect Part A of Fig. 11. That means, the push-pull fume cupboard should be operated in Part A to avoid the effect of walk-by.

ACKNOWLEDGEMENTS

We highly appreciate the financial support from National Science Council Taiwan (Gant No. NSC 96-2221-E-011-098-MY3).

REFERENCES

ASHRAE (1995) *Method of Testing Performance Laboratory Fume Hood, ANSI/ASHRAE 110-1995*,.Atlanta, GA, USA.

Battista, W.P. (1947) Semi-lateral tank ventilation cupboard controls contamination, cut costs. *Heat Piping Air Condition* 19: 85-89.

Chern, M.J. and Ma, C.H. (2007) Numerical investigation and recommendations for push-pull ventilation systems. *Journal of Occupational and Environmental Hygiene* 31: 505-512.

Chern, M.J. and Cheng, W.Y. (2007) Numerical investigation of turbulent diffusion in push-pull and exhaust fume cupboards. *Annals of Occupational Hygiene* 51: 517 - 531.

Hama, G.M. (1957) Supply and exhaust ventilation for metal picking operations. *Air Condition, Heat Ventilation* 54: 61-63.

Huang, R.F. *et al.* (2005) Aerodynamic characteristics and design guidelines of push-pull ventilation systems. *Annals of Occupational Hygiene* 49: 1-15.

Huang, R.F., Lin, S.Y., Jan, S.Y., Chen, Y.K., Chen, C.W., Yeh, W.Y., Chang, C.P., Shih, T.S., Chen, C.C. (2005) Aerodynamic characteristics and design guidelines of push-pull ventilation systems. *Annals of Occupational Hygiene* 49: 1-15.

Malin, B.S. (1945) Practical pointers on industrial exhaust systems. *Heat and Ventilation* 42: 75-82

Robinson, M. and Ingham, D.B (1995a) Numerical modeling of the flow patterns induced by a push-pull ventilation system. *Annals of*

Occupational Hygiene 40: 293-310.
Robinson, M. and Ingham, D.B. (1995b) Recommendations for the design of push-pull ventilation systems for open surface tanks. *Annals of Occupational Hygiene* 40: 693-704.
Rota, R., Nano, G. and Canossa, L. (2001) Design guidelines for push-pull ventilation systems thourgh computational fluid dynamics modeling. *AIHA Journal* 62: 141-148.